

Increased carbonylation, protein aggregation and apoptosis in the spinal cord of mice with experimental autoimmune encephalomyelitis

Anushka Dasgupta*, Jianzheng Zheng*, Nora I. Perrone-Bizzozero† and Oscar A. Bizzozero*¹

*Department of Cell Biology and Physiology, University of New Mexico Health Sciences Center, Albuquerque, NM, U.S.A.

†Department of Neurosciences, University of New Mexico Health Sciences Center, Albuquerque, NM, U.S.A.

Cite this article as: Dasgupta A, Zheng J, Perrone-Bizzozero NI, Bizzozero OA (2013) Increased carbonylation, protein aggregation and apoptosis in the spinal cord of mice with experimental autoimmune encephalomyelitis. ASN NEURO 5(2):art:e00111.doi:10.1042/AN20120088

ABSTRACT

Previous work from our laboratory implicated protein carbonylation in the pathophysiology of both MS (multiple sclerosis) and its animal model EAE (experimental autoimmune encephalomyelitis). Subsequent *in vitro* studies revealed that the accumulation of protein carbonyls, triggered by glutathione deficiency or proteasome inhibition, leads to protein aggregation and neuronal cell death. These findings prompted us to investigate whether their association can be also established *in vivo*. In the present study, we characterized protein carbonylation, protein aggregation and apoptosis along the spinal cord during the course of MOG (myelin-oligodendrocyte glycoprotein)_{35–55} peptide-induced EAE in C57BL/6 mice. The results show that protein carbonyls accumulate throughout the course of the disease, albeit by different mechanisms: increased oxidative stress in acute EAE and decreased proteasomal activity in chronic EAE. We also show a temporal correlation between protein carbonylation (but not oxidative stress) and apoptosis. Furthermore, carbonyl levels are significantly higher in apoptotic cells than in live cells. A high number of juxta-nuclear and cytoplasmic protein aggregates containing the majority of the oxidized proteins are present during the course of EAE. The LC3 (microtubule-associated protein light chain 3)-II/LC3-I ratio is significantly reduced in both acute and chronic EAE indicating reduced autophagy and explaining why aggregates accumulate in this disorder. Taken together, the results of

the present study suggest a link between protein oxidation and neuronal/glial cell death *in vivo*, and also demonstrate impaired proteostasis in this widely used murine model of MS.

Key words: apoptosis, autophagy, experimental autoimmune encephalomyelitis, oxidative stress, protein aggregation, protein carbonylation, proteostasis

INTRODUCTION

EAE (experimental autoimmune encephalomyelitis) is an animal model of MS (multiple sclerosis) that is routinely used to study the mechanistic basis of disease and to test therapeutic approaches (Gold et al., 2000). Both disorders are characterized by CNS (central nervous system) inflammation, demyelination and axonal degeneration, and various degrees of oligodendrocyte and neuronal cell death (Lucchinetti et al., 1996; Kornek and Lassmann, 1999; Kuerten et al., 2007). In recent years, several laboratories have obtained experimental evidence indicating that oxidative stress is a major player in the pathogenesis of inflammatory demyelination (Gilgun-Sherki et al., 2004; Bizzozero, 2009; Haider et al., 2011). Severe and/or prolonged oxidative stress conditions do lead to the non-enzymatic modification of specific amino acid residues resulting in the introduction of aldehyde or ketone functional groups (also known as carbonylation)

¹To whom correspondence should be addressed (email obizzozero@salud.unm.edu).

Abbreviations: AMC, 7-aminomethyl-4-coumarin; APC, adenomatous polyposis coli protein C-terminus; CFA, complete Freund's adjuvant; CNS, central nervous system; DAPI, 4',6-diamidino-2-phenylindole; DNP, 2,4-dinitrophenyl; DNPH, 2,4-dinitrophenylhydrazine; DPI, days post-immunization; EAE, experimental autoimmune encephalomyelitis; ECL, enhanced chemiluminescence; GFAP, glial fibrillary-associated protein; HRP, horseradish peroxidase; LC3, microtubule-associated protein light chain 3; MOG, myelin-oligodendrocyte glycoprotein; MS, multiple sclerosis; TBARS, thiobarbituric acid-reacting substances; TUNEL, terminal deoxynucleotidyltransferase-mediated dUTP nick-end labelling.

© 2013 The Author(s) This is an Open Access article distributed under the terms of the Creative Commons Attribution Non-Commercial Licence (NC-BY) (<http://creativecommons.org/licenses/by-nc/2.5/>) which permits unrestricted non-commercial use, distribution and reproduction in any medium, provided the original work is properly cited.

(Stadtman and Berlett, 1997). Thus it is not surprising that large amounts of carbonylated proteins accumulate within CNS cells in many neurodegenerative disorders (Ferrante et al., 1997; Floor and Wetzel, 1998; Aksenov et al., 2001; Perluigi et al., 2005), as well as in neuroinflammatory disorders such as MS (Bizzozero et al., 2005) and EAE (Smerjac and Bizzozero, 2008; Zheng and Bizzozero, 2010a). However, the build-up of oxidized and other misfolded proteins is due not only to an increase in the rate of protein oxidation, but also to their reduced proteolytic removal via the proteasome (Shringarpure et al., 2001; Divald and Powell, 2006). In fact, impaired proteasomal activity has been demonstrated in disorders where carbonylated proteins accumulate, including Alzheimer's disease (Keller et al., 2000), Parkinson's disease (McNaught et al., 2003), Huntington's disease (Seo et al., 2004) and more recently in MS (Zheng and Bizzozero, 2011) and EAE (Zheng and Bizzozero, 2010b; Zheng et al., 2012).

There is a substantial amount of data showing that the presence of carbonyl groups causes major changes in protein structure and function (Fucci et al., 1983; Starke et al., 1987; Dalle-Donne et al., 2001), which results in the loss of cell viability (England et al., 2004; Magi et al., 2004). In addition, carbonylation brings about the formation of protease-resistant protein aggregates, which are considered highly toxic and can mediate cell death (Nyström, 2005; Maisonneuve et al., 2008b). Indeed, we have recently shown that protein carbonylation, aggregation and cell death are linked during neuronal apoptosis triggered by glutathione deficiency (Dasgupta et al., 2012). These findings and the fact that both protein oxidation (Smerjac and Bizzozero, 2008; Zheng and Bizzozero, 2010a) and neuronal/oligodendrocyte apoptosis has been observed in EAE (Meyer et al., 2001; Das et al., 2008), prompted us to investigate whether their association can be also established *in vivo*. In the present study, and as a first step to demonstrate such a relationship, we measured the extent of protein carbonylation, protein aggregation and apoptosis along the spinal cord of mice with acute and chronic EAE. The results show for the first time (i) a temporal correlation between protein carbonylation (but not oxidative stress) and apoptosis, (ii) increased accumulation of carbonyls in apoptotic cells, (iii) the presence in EAE of protein aggregates containing the majority of the oxidized proteins, and (iv) reduced autophagy in both acute and chronic EAE, which suggests impaired proteostasis in this murine model of MS. A preliminary account of these findings has been presented in abstract form (Dasgupta and Bizzozero, 2011).

MATERIAL AND METHODS

Induction of EAE

Housing and handling of the animals, as well as the euthanasia procedure, were in strict accordance with the NIH

(National Institutes of Health) Guide for the Care and Use of Laboratory Animals, and were approved by the Institutional Animal Care and Use Committee. Eight-week-old female C57BL/6 mice were purchased from Harlan Bioproducts and housed at the UNM (University of New Mexico) animal resource facility. EAE was induced by active immunization with MOG (myelin-oligodendrocyte glycoprotein)_{35–55} peptide (AnaSpec) as described previously (Zheng and Bizzozero, 2010a). Animals were weighed and examined daily for the presence of neurological signs. Acute disease was defined as having maximal neurological symptoms of EAE without any improvement for at least three consecutive days, whereas chronic EAE was operationally defined as animals that remain in the stationary phase of the disease for 30 days. Age-matched control animals for acute EAE (control young) and chronic EAE (control old) consisted of mice injected with CFA (complete Freund's adjuvant) alone (i.e. without the MOG peptide). EAE and control mice were killed by decapitation, and the spinal cord was rapidly removed and divided into cervical, thoracic and lumbar regions. Sections were either fixed with methacarn (methanol/chloroform/acetic acid, 60:30:10, by vol.) or homogenized in PEN buffer [20 mM sodium phosphate (pH 7.5), 1 mM EDTA and 0.1 mM neocuproine] containing 2 mM 4,5 dihydroxy-1,3-benzene disulfonic acid and 1 mM dithiothreitol. Protein homogenates were stored at -80°C until use. The protein concentration was assessed with the Bio-Rad DCTTM protein assay (Bio-Rad Laboratories) using BSA as a standard. For GSH determination, homogenates were prepared in PEN buffer without reducing agents and were processed immediately as described below.

Determination of GSH and lipid peroxidation products

GSH levels were determined using the enzymatic recycling method (Shaik and Mehvar, 2006). Briefly, proteins from spinal cord homogenates were precipitated with 1% sulfosalicylic acid and removed by centrifugation at 10000 *g* for 15 min. Aliquots of the supernatant were then incubated with 0.4 unit/ml glutathione reductase, 0.2 mM NADPH and 0.2 mM 5,5'-dithiobis-(2-nitrobenzoic acid) in 1 ml of 0.2 M sodium phosphate buffer (pH 7.5) containing 5 mM EDTA. The rate of appearance of the thionitrobenzoate anion was measured spectrophotometrically at 412 nm. [GSH] was calculated by interpolation on a curve made with increasing concentrations of GSSG (0.1–10 nmol).

Lipid peroxidation was estimated as the amount of TBARS (thiobarbituric acid-reacting substances) (Ohkawa et al., 1979). Briefly, aliquots from the spinal cord homogenates were suspended in 10% (w/v) trichloroacetic acid containing 1% (w/v) thiobarbituric and 0.05% butylated hydroxytoluene. Samples were incubated for 20 min at 90°C . Aggregated material was removed by centrifugation at 10000 *g* for 15 min and the absorbance of the supernatant was measured at 532 nm. The amount of TBARS was calculated using a standard curve prepared with 1,1,3,3-tetraethoxypropane.

Proteasome and calpain activity

The chymotrypsin-like activity of the 20S proteasome in the spinal cord homogenates was determined using a fluorescence assay (Rodgers and Dean, 2003). Briefly, 50 μg of protein was incubated for up to 2 h at 25 °C with 50 μM of the AMC (7-aminomethyl-4-coumarin)-labelled peptide Suc-Leu-Leu-Val-Tyr-AMC in the absence or presence of 10 μM β -clasto-lactacystin-lactone (Enzo Life Sciences). The proteasome activity was calculated as the difference in fluorescence intensity at 460 nm between the samples without and with inhibitor using an excitation wavelength of 380 nm. Calpain activity was also determined with a fluorescence assay using the substrate Suc-Leu-Leu-Val-Tyr-AMC in 100 mM KCl, 10 mM CaCl_2 and 25 mM Hepes buffer (pH 7.5), and carrying out the incubation in the absence or presence of 40 $\mu\text{g}/\text{ml}$ calpeptin (Hassen et al., 2006).

Oxyblot analysis

Protein carbonyl groups were measured by oxyblot analysis as described previously (Smerjac and Bizzozero, 2008). In brief, proteins (5 μg) were incubated with DNPH (2,4-dinitrophenylhydrazine) to form the DNP (2,4-dinitrophenyl) hydrazone derivatives. Proteins were separated by electrophoresis and blotted on to PVDF membranes. DNP-containing proteins were detected using rabbit DNP antiserum (1:500 dilution) and HRP (horseradish peroxidase)-conjugated goat anti-rabbit IgG antibody (1:2000 dilution). Blots were developed by ECL (enhanced chemiluminescence) using the Western Lightning ECL™ kit from PerkinElmer. Films were scanned in a Hewlett Packard Scanjet 4890 and the images were quantified using the NIH Image 1.63 imaging analysis program. The intensity of each lane on the film was normalized by the amount of Coomassie Blue staining in the corresponding lane.

Immunohistochemistry

Tissue specimens were fixed overnight in methacarn and then embedded in paraffin. Tissue was cross-sectioned (3- μm thick) and mounted on Vectabond™-treated slides (Vector Laboratories). Sections were deparaffinized with xylenes and a graded alcohol series, and then rinsed with PBS solution for 10 min. Apoptosis was detected using Click-iT® TUNEL (terminal deoxynucleotidyltransferase-mediated dUTP nick-end labelling) Assay kit (Invitrogen). For carbonyl staining, sections were incubated for 15 min with 1 mg/ml DNPH prepared in 1 M HCl to convert carbonyl groups into DNP-hydrazones. Sections were rinsed three times with PBS, blocked with 10% (v/v) normal goat serum and incubated overnight with rabbit anti-DNP antibody (1:1000 dilution) (Sigma). After removing the primary antibody with 0.1% Triton X-100 in PBS, sections were incubated for 3 h with Alexa Fluor® 647-conjugated goat anti-rabbit antibody (1:200 dilution) (Molecular Probes). Sections were rinsed twice with PBS, and then mounted us-

ing DPX. Images were captured with a Zeiss 200m microscope (Carl Zeiss MicroImaging) equipped with a Hamamatsu C4742-95 digital camera.

For double immunofluorescence, DNPH-treated sections were incubated with the corresponding primary antibody, washed with PBS, followed by incubation with fluorescent secondary antibodies (Alexa Fluor® 647-conjugated, 1:200 dilution) (Molecular Probes). After washing, the sections were stained using the Click-iT® TUNEL Assay kit (Invitrogen), rinsed with PBS and mounted using DPX. The various cell types were detected by using antibodies against GFAP (glial fibrillary-associated protein) (1:250 dilution, mouse monoclonal; Sigma), APC (adenomatous polyposis coli protein C-terminus) (1:100, mouse monoclonal, Chemicon) and NeuN (1:200, mouse monoclonal, Chemicon) with a corresponding secondary antibody conjugated to Alexa Fluor® 488.

For protein aggregation staining, methacarn-fixed and paraffin-embedded tissue sections were deparaffinized and hydrated followed by washing with PBS. Samples were then incubated for 30 min with ProteoStat® Protein Aggregation Assay solution (Enzo Life Sciences) and destained using distilled water for 5 h. Cellular nuclei were stained with DAPI (4',6-diamidino-2-phenylindole; 40 ng/ml, Sigma). Stained sections were mounted using 1,4-diazabicyclo[2.2.2]octane in poly(vinyl alcohol) (Sigma) as antifading agent.

Determination of the autophagy index

Proteins (7.5 μg) were separated by SDS/PAGE on 15% gels and blotted on to PVDF membranes. LC3 (microtubule-associated protein light chain 3)-I (18 kDa) and LC3-II (16 kDa) were detected using rabbit LC3 antiserum (1:1000 dilution, Sigma) and HRP-conjugated goat anti-rabbit IgG antibody (1:2000 dilution). Blots were developed by ECL as described above. The LC3-II/LC3-I ratio was determined by scanning densitometry of the films.

Protein aggregation assay

Assessment of protein aggregation was carried out as described by Maisonneuve et al. (2008a) with minor modifications. Spinal cord homogenates prepared in PEN buffer containing 1 mM dithiothreitol and 150 mM NaCl were centrifuged at 20000 *g* for 30 min at 4 °C. The pellets were then extracted with the same buffer containing 1% Triton X-100. Samples were kept on ice for 15 min and then centrifuged at 20000 *g* for 30 min at 4 °C. The final pellet, which contains some cytoskeleton structures but mostly aggregated proteins, was processed for oxyblot analysis as described above.

Statistical analysis

Results were analysed for statistical significance with Student's *t* test using the GraphPad Prism® program (GraphPad Software).

RESULTS

Characteristics of mice with acute and chronic EAE

EAE in female C57BL/6 mice was induced by active immunization with MOG_{35–55} peptide as described in the Materials and methods section. Symptoms were graded according to the following scale: 0, no symptoms; 1, tail weakness; 1.5, clumsy gait; 2, hind-limb paresis; 2.5, partial hind-limb dragging; 3, hind-limb paralysis; 3.5, hind-limb paralysis with fore-limb paresis; 4, complete paralysis; and 5, moribund. In this EAE model, neurological symptoms begin at 14 DPI (days post-immunization) (i.e. 7 days after the boost with MOG peptide) reaching a peak at 30 DPI, and most animals remain ill throughout the entire experimental period (60 DPI). Acute disease was defined as having maximal neurological symptoms of EAE without any improvement for at least 3 consecutive days. At this stage the spinal cord pathology is characterized by infiltration of inflammatory cells, mostly within the white matter and meninges. Chronic EAE was defined arbitrarily as animals that remain in the stationary phase of the disease for 30 days (60 DPI). At this stage there is very low perivascular and parenchymal inflammation, and almost no transmigration of inflammatory cells into the spinal cord. CFA-injected animals, which were killed at 30 DPI (control young) and 60 DPI (control old), did not exhibit any neurological sign or spinal cord pathology. For the present study we analysed a total of 29 animals: six control-young, 11 acute EAE (clinical scores ranging from 1.0 to 3.5), six control-old and six chronic EAE (clinical scores ranging from 0.5 to 3.5) (Figure 1a).

Increased neuronal and glial apoptosis in the spinal cord of mice with acute and chronic EAE

Using TUNEL staining we first measured the number of cells undergoing apoptosis in different spinal cord regions (cervical, thoracic and lumbar) during the course of EAE. As shown in Figure 1, the total number of apoptotic cells in the spinal cord of mice with acute EAE (Figure 1b) was slightly higher than that with chronic EAE (Figure 1c). In both cases, the lumbar section showed the highest number of apoptotic cells, followed by the thoracic and cervical sections. These findings are in agreement with the notion that the extent of spinal cord lesions increases caudally (Müller et al., 2000). Similar results were obtained using active caspase 3 as a marker of apoptosis (data not shown).

Double staining of the lumbar spinal cord sections of acute EAE mice for TUNEL and cell-specific markers identified apoptotic cells as oligodendrocytes (48%), neurons (27%) and astrocytes (15%) (Figures 2a and 2b). The identity of the remaining apoptotic cells (probably microglia and lympho-

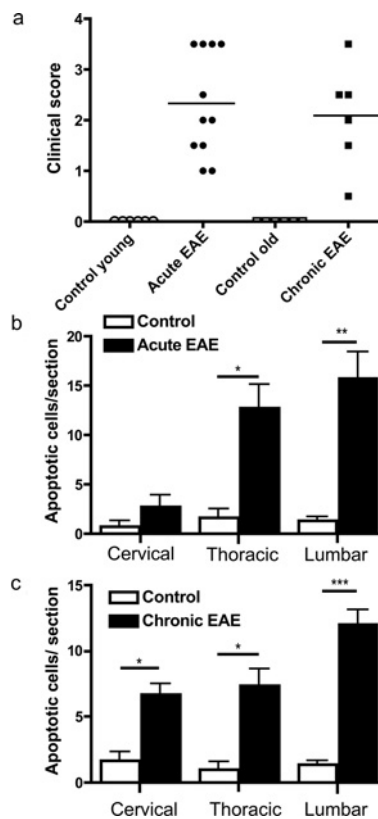


Figure 1 Apoptosis along the spinal cord is high in both acute and chronic EAE

(a) Clinical scores of animals used in the present study. (b and c) Number of apoptotic cells determined by TUNEL staining in the different spinal cord regions (cervical, thoracic and lumbar) of acute and chronic EAE mice respectively. A total of five to eight non-consecutive (30 μ m apart) 3- μ m-thick sections per animal were analysed and averaged. Values represent the means \pm S.E.M. for three animals per experimental group. Clinical scores (means \pm S.E.M.) of acute and chronic EAE mice were 2.2 ± 0.7 and 1.8 ± 0.7 respectively. * $P < 0.05$, ** $P < 0.005$, *** $P < 0.0005$.

cytes) was not determined. A similar distribution was found in chronic EAE animals, where 45, 20 and 13% of the apoptotic cells were identified as oligodendrocytes, neurons and astrocytes respectively. Stereological analysis of the same spinal cord region revealed that there was 27% neuronal loss, 15% oligodendrocyte loss and 36% increase in the number of astrocytes (astrocytosis) in acute EAE (Figure 2c). In chronic EAE, neuronal and oligodendrocyte deficits were 29% and 21% respectively, whereas astrocyte number was almost unchanged (Figure 2d).

Protein carbonylation, and not oxidative stress, correlates with apoptosis

As shown in Figure 3(a), GSH levels were reduced in all regions of the spinal cord of mice with acute EAE, with the largest decline (~46%) found in the lumbar section.

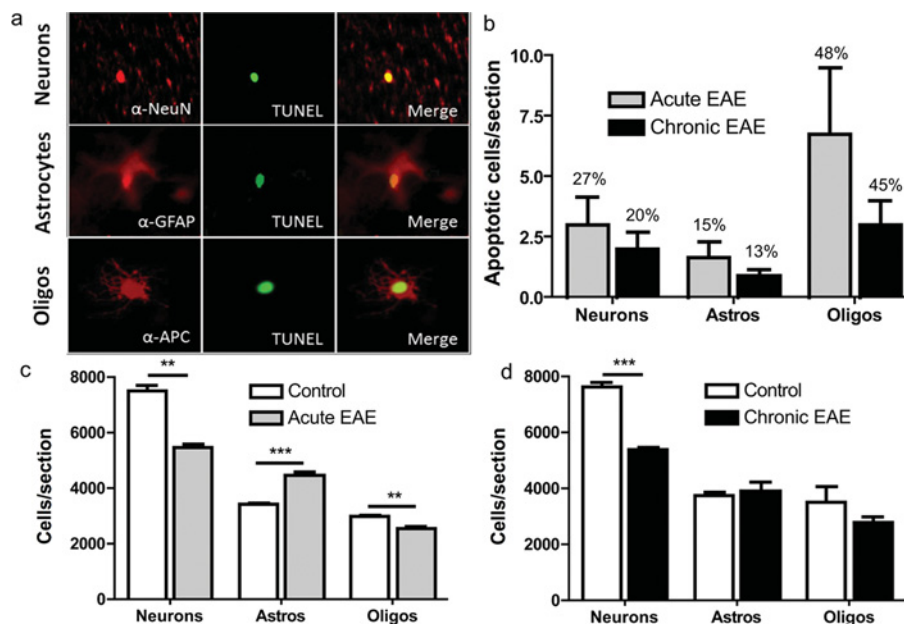


Figure 2 Significant neuronal and glial apoptosis occurs in acute and chronic EAE

(a) High-magnification double-label immunofluorescence images of lumbar spinal cord sections of acute EAE mice depicting an apoptotic neuron, astrocyte and oligodendrocyte. Immunohistochemical detection of cellular apoptosis was determined using TUNEL (green channel) and antibodies against specific cell types (NeuN for neurons, GFAP for astrocytes and APC for oligodendrocytes). (b) Number of TUNEL-positive cells in the lumbar spinal cord of acute and chronic EAE mice that are identified as neurons, astrocytes and oligodendrocytes. A total of five non-consecutive (30 μ m apart) 0.3- μ m-thick sections per animal were analysed and averaged. Values are the means \pm S.E.M. for three to six animals per experimental group. Clinical scores (means \pm S.E.M.) of acute and chronic EAE mice were 2.2 ± 0.7 and 1.8 ± 0.7 respectively. Numbers on top of the bars are the values expressed as the percentages of TUNEL-positive cells. Note that the numbers do not add up to 100% since there are other unidentified apoptotic cells. (c and d) Average number of neurons, astrocytes and oligodendrocytes per section in the lumbar spinal cord region of acute and chronic EAE mice respectively. Cells were identified using the same markers as indicated above and DAPI staining. A total of five non-consecutive (30 μ m apart) 3- μ m-thick sections per animal were analysed and averaged. Values represent the means \pm S.E.M. for three mice per experimental group. ** $P < 0.005$, *** $P < 0.0005$.

In contrast, normal GSH concentrations were present in all of the spinal cord areas of animals with chronic EAE (Figure 3b). These data are consistent with a weakened cellular antioxidant defence system in acute EAE where inflammation is elevated. In agreement with the GSH data, levels of TBARS, a marker of lipid peroxidation, were elevated in all spinal cord segments of acute EAE (Figure 3c), but not chronic EAE (Figure 3d) mice. Certainly, there was an almost perfect inverse relationship between GSH and TBARS levels throughout the length of the spinal cord. In contrast with lipid peroxidation, the amount of protein carbonyls was augmented in both acute EAE (Figure 4a) and chronic EAE (Figure 4b) spinal cord with the highest increase found in the lumbar area. Since protein carbonyls are not eliminated by enzymatic reduction to the corresponding alcohols (Bizzozero, 2009), the accumulation of protein carbonyls in chronic EAE in the absence of significant oxidative stress is most likely to be due to impaired proteolytic removal via the chymotrypsin-like activity of 20S proteasome (Ferrington et al., 2005). Indeed, this proteasomal activity, measured with a fluorogenic peptide substrate, was found to be normal in acute EAE mice (Figure 4c), but

greatly decreased in all spinal cord regions of chronic EAE mice (Figure 4d).

Apoptotic cells contain higher levels of protein carbonyls

Since protein carbonylation and cell death shows a similar temporal pattern, we sought to investigate whether there is a spatial relationship between these two parameters as well. To this end, spinal cord sections were double-stained with DNPH for carbonyls and TUNEL for apoptosis. Co-localization studies of carbonyls and annexin V, a late marker in the apoptotic pathway, were not possible since sections for carbonyl detection had to be fixed in methacarn, which dissolves membrane phospholipids. Figure 5 shows that apoptotic (TUNEL-positive) cells are stained intensely with DNPH. Since this reagent also stains cell nuclei, probably due to its reactivity towards DNA oligonucleotides (Luo and Wehr, 2009), only the fluorescence present in the cytoplasm was quantified. As shown in Figure 5(c), the fluorescence intensity in the cytoplasm of apoptotic cells from the lumbar spinal cord region

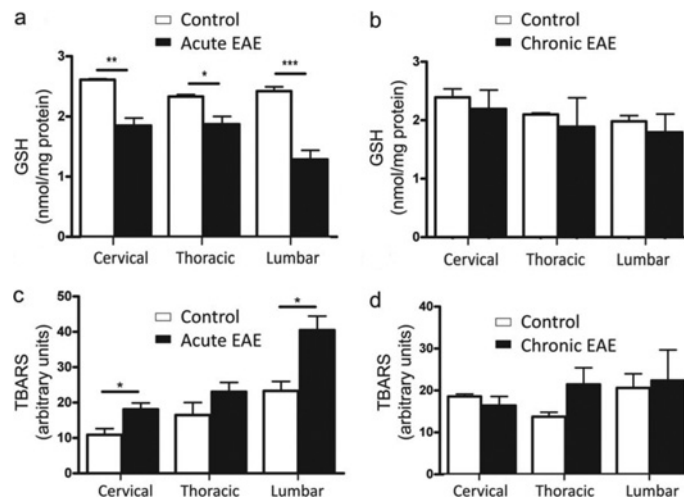


Figure 3 Diminished GSH levels and increased lipid peroxidation are found only in acute EAE (a and b) GSH levels in the various spinal cord regions (cervical, thoracic and lumbar) of acute and chronic EAE mice respectively. Values represent the means \pm S.E.M. for three to four animals per experimental group. Clinical scores (means \pm S.E.M.) of acute and chronic EAE mice were 2.0 ± 0.5 and 1.7 ± 0.6 respectively. (c and d) TBARS levels in the different spinal cord regions of acute and chronic EAE mice respectively. Values represent the means \pm S.E.M. for three to five animals per experimental group. Clinical scores (means \pm S.E.M.) of acute and chronic EAE mice were 2.3 ± 0.5 and 1.7 ± 0.6 respectively. * $P < 0.05$, ** $P < 0.005$, *** $P < 0.0005$.

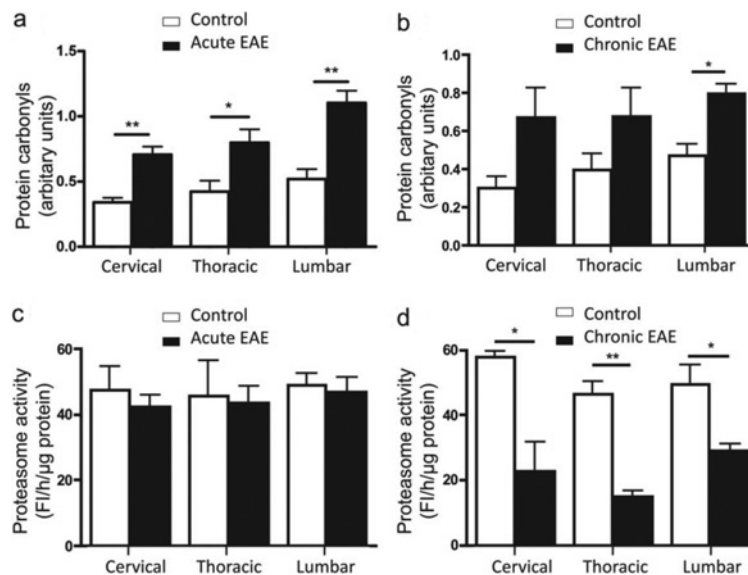


Figure 4 Protein carbonyls accumulate in both acute and chronic EAE (a and b) Protein carbonyl levels in the various spinal cord regions (cervical, thoracic and lumbar) of acute and chronic EAE mice respectively. (c and d) Proteasome chymotrypsin-like activity in the different spinal cord regions of acute and chronic EAE mice respectively. FI, fluorescence units. Values represent the means \pm S.E.M. for three animals per experimental group. Clinical scores (means \pm S.E.M.) of acute and chronic EAE mice were 2.2 ± 0.7 and 1.8 ± 0.7 respectively. * $P < 0.05$, ** $P < 0.005$.

of mice with acute EAE was ~ 2 -fold higher than that of non-apoptotic cells.

Carbonyls accumulate in all of the major cell types of EAE spinal cord

Carbonyl levels in the various CNS cell types were determined by double-label immunofluorescence using

antibodies against NeuN, APC and GFAP to identify neurons, oligodendrocytes and astrocytes respectively. Carbonyl intensity in the control lumbar spinal cord region was the highest in astrocytes (150.7 ± 8.3) followed by oligodendrocytes (94.9 ± 6.7) and neurons (21.0 ± 1.3) (Figure 6). In acute EAE, carbonyl intensity in astrocytes, oligodendrocytes and neurons increased 2.8-, 2.1- and 4.3-fold respectively. This suggests the occurrence of different oxidative

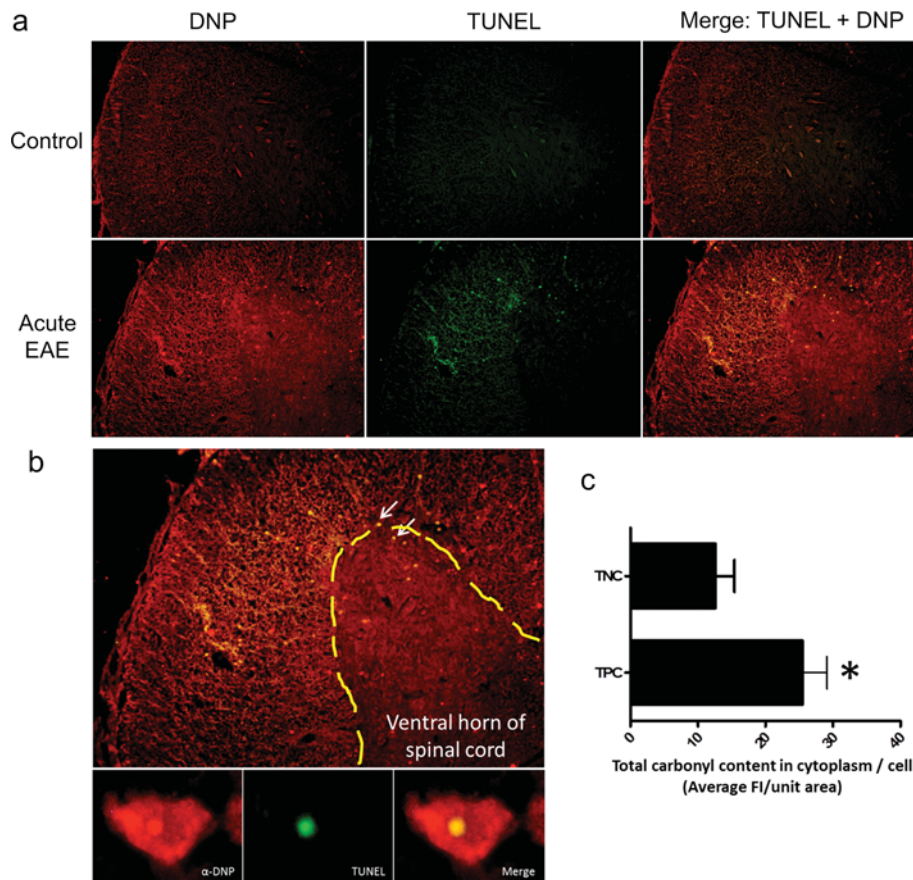


Figure 5 Carbonylation levels are higher in apoptotic than in non-apoptotic cells
 (a) Double-label immunofluorescence images of lumbar spinal cord sections from control and acute EAE mice. Carbonyls were detected by anti-DNP labelling after derivatization with DNPH (red channel) and apoptotic cells were identified by TUNEL staining (green channel). (b) High-magnification image depicting a TUNEL-positive cell containing extensive carbonyl staining in the cytoplasm. (c) Histogram showing carbonyl levels in the cytoplasm of TUNEL-positive cells (TPC) and TUNEL-negative cells (TNC) in the lumbar spinal cord region of acute EAE mice. A total of ten non-consecutive (30 μm apart) 3-μm-thick sections per animal were analysed and averaged. Values represent the means ± S.E.M. for five animals per experimental group. Clinical scores (means ± S.E.M.) of acute EAE mice were 2.3 ± 0.5. **P* < 0.05. FI, fluorescence intensity.

environments and/or proteasome activities in the various cell types.

The number of large protein aggregates is also increased in EAE

Experiments were also conducted to determine the possible association between protein aggregation and cell death. Unfortunately, simultaneous staining for TUNEL and protein aggregation (ProteoStat®) was not possible due to the overlapping emission spectrum of the dyes in the corresponding kits. Nonetheless, we found a significant increase in the number of protein aggregates, both juxta-nuclear (aggresomes) and cytoplasmic, in all three spinal cord areas of mice with acute EAE as compared with controls (Figures 7a and 7b). The EAE lumbar section had the largest number of aggregates, followed by the thoracic and cervical spinal cord regions. A similar pattern was observed in chronic EAE, except that the

amount of protein aggregates in all three spinal cord areas was higher than those measured in acute EAE (Figure 7c). Furthermore, in acute EAE, linear regression curves predicted a positive relationship between all three: protein carbonylation ($r^2 = 0.97$), protein aggregation ($r^2 = 0.83$) and cell death ($r^2 = 0.88$) and the clinical score (Figure 7d). The presence of aggresomes in EAE also suggested an impairment of autophagy, the major degradation system responsible for the turnover of bulky cellular components. Indeed, we found that the LC3-II/LC3-I ratio (also known as the autophagy index) was significantly reduced in both acute and chronic EAE (Figure 8).

Most carbonylated proteins are present in insoluble protein aggregates

To determine whether carbonylated proteins are part of protein aggregates, we fractionated the spinal cord

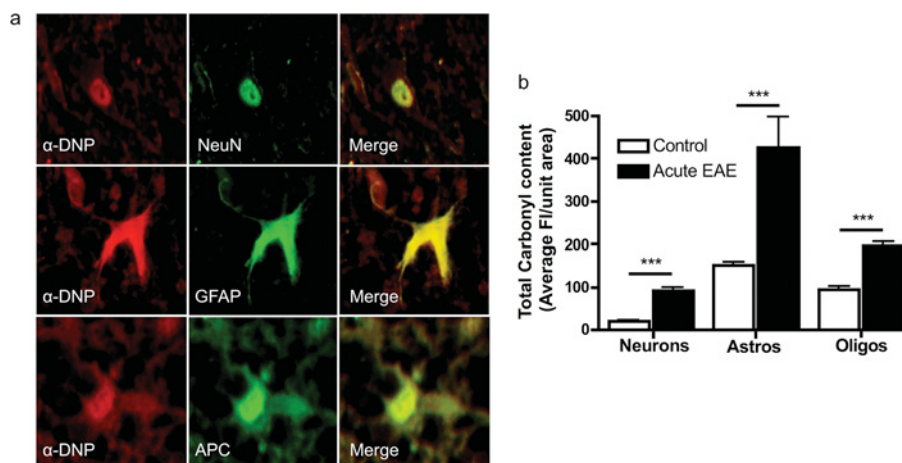


Figure 6 Carbonyls accumulate in all of the major cell types present in the EAE spinal cord (a) Double-label immunofluorescence images of cells from the lumbar spinal cord region of acute EAE mice depicting carbonyl staining in the red channel (anti-DNP labelling after derivatization with DNPH) and cell-type markers in the green channel (NeuN for neurons, GFAP for astrocytes and APC for oligodendrocytes). (b) Carbonyl content in different cell types in the lumbar spinal cord of control and acute EAE mice. A total of five to eight non-consecutive (30 μ m apart) 3- μ m-thick sections per animal were analysed and averaged. Values represent the means \pm S.E.M. for five animals per experimental group. Clinical scores (means \pm S.E.M.) of acute EAE mice were 2.3 ± 0.5 . *** $P < 0.0005$. FI, fluorescence intensity.

homogenates by differential centrifugation as described by Maisonneuve et al. (2008a). This method is based on the large sedimentation coefficient of protein aggregates relative to other cellular protein complexes and on their insolubility in high-ionic-strength buffers containing the non-denaturing detergent Triton X-100. As shown in Figure 9, carbonylated proteins were highly enriched in the detergent-insoluble protein fraction both in control and EAE samples. It is of note that the Triton-insoluble fraction, which has less than 20% of the protein present in the initial spinal cord homogenate, contained between 60 and 70% of the carbonylated proteins. These data suggest that, like in other aerobic systems (Maisonneuve et al., 2008b), oxidized proteins are the major substrates for aggregation.

DISCUSSION

The present study reveals a positive correlation between protein carbonylation (but not oxidative stress) and neuronal and glial apoptosis in the spinal cord of EAE mice. As we found in glutathione-depleted or proteasome-inhibited cultured neurons (Dasgupta et al., 2012), apoptotic cells have increased carbonyl accumulation, suggesting a cytotoxic role for this modification. We also describe for the first time the presence of protein aggregates in EAE, which contain the majority of the oxidized proteins. Furthermore, the build-up of these inclusion bodies may result not only from augmented carbonylation, but also from reduced clearance by autophagy. The proteasome deficiency in chronic EAE and the decrease

in autophagy in both acute and chronic EAE clearly points to an impaired proteostasis in this murine model of inflammatory demyelination. A schematic model summarizing our experimental findings is shown in Figure 10.

Consistent with previous studies (Pender et al., 1991; Akassoglou et al., 1998; Anderson et al., 2008; Vogt et al., 2009; Toft-Hansen et al., 2011) we found significant neuronal and oligodendrocyte loss in acute EAE along with astrocytosis. The latter involves astrocyte activation, hypertrophy and proliferation, which are considered to be a characteristic response to inflammation or autoimmune injury of the CNS (Toft-Hansen et al., 2011). Interestingly, the extent of neuronal and oligodendrocyte loss in chronic EAE is similar to that in acute EAE, despite apoptosis continuing throughout the disease process. Although oligodendrocytes have some regenerating capacity that could explain these findings (Arenella and Herndon, 1984; Tripathi et al., 2010), the mitotic rate of neurons is almost nil (Tripathi et al., 2010). Thus we can conclude that (i) the majority of neurons, and possibly oligodendrocytes, die during the acute (inflammatory) phase, and (ii) only a small, yet significant, fraction of cell death occurs by apoptosis. The notion that most cell death occurs early in the disease is supported by the finding that calpain activity, a marker of both necrosis and apoptosis (Guyton et al., 2005), is elevated in acute EAE, but not in chronic EAE (Supplementary Figure S1 at <http://www.asnneuro.org/an/005/an005e111add.htm>).

Like in most neurodegenerative disorders, oxidative stress is also a significant player in the pathogenesis of inflammatory demyelination (Smith et al., 1999; Gilgun-Sherki et al., 2004). At the peak of the disease, and concomitant with the rise in inflammation, there is increased oxidative stress

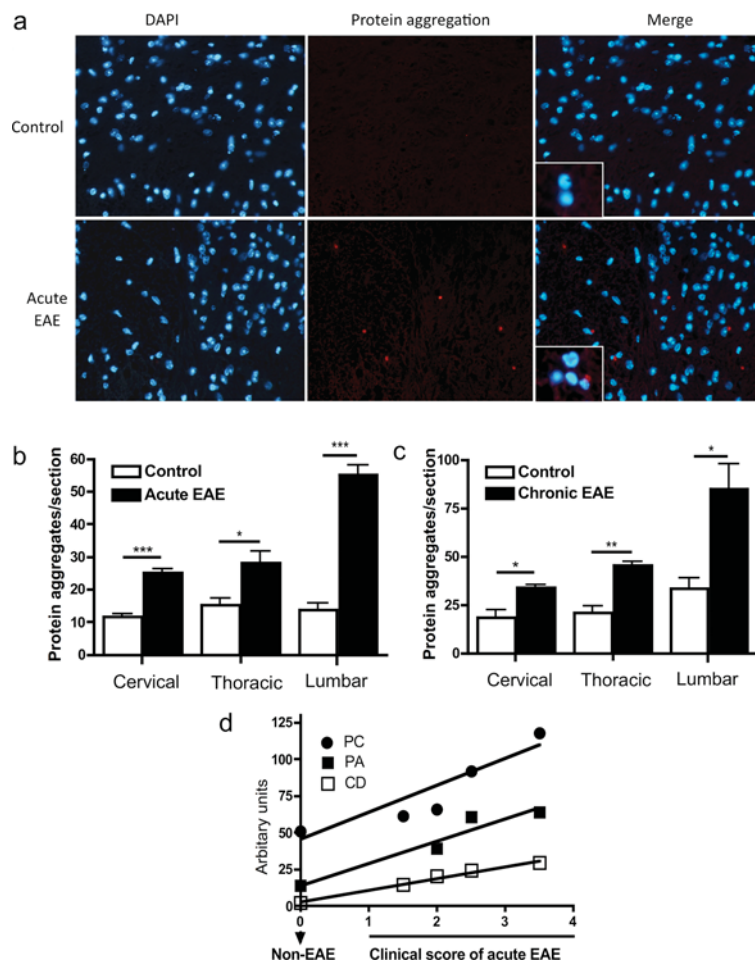


Figure 7 The number of protein aggregates augments in both acute and chronic EAE

(a) Representative images of lumbar spinal cord of control and acute EAE mice stained with the ProteoStat[®] protein aggregation dye (red) and DAPI (light blue) for nuclear identification. (b and c) Histograms showing the number of large protein aggregates in cross-sections of the various spinal cord regions from mice with acute and chronic EAE respectively. A total of 9–15 non-consecutive (30 μ m apart) 3- μ m-thick sections per animal were analysed and averaged. Values represent the means \pm S.E.M. for three to five animals per experimental group. Clinical scores (means \pm S.E.M.) of acute and chronic EAE mice were 2.4 ± 0.5 and 2.5 ± 0.6 respectively. (d) Linear regression curves predicting a positive relationship between protein carbonylation (PC, $r^2 = 0.97$), protein aggregation (PA, $r^2 = 0.83$) and cell death (CD, $r^2 = 0.88$) with the clinical score. Each point represents the average of two to three EAE mice per experimental group.

with the ensuing depletion of cellular GSH and accumulation of lipid peroxides and protein carbonyls. There are several, and not mutually exclusive, reasons underlying the reduction in GSH in acute EAE. These include (i) oxidation of GSH to glutathione disulfide (GSSG); (ii) conjugation of GSH with reactive α,β -unsaturated aldehydes derived from lipid peroxidation (e.g. acrolein, 4-hydroxynonenal); (iii) reduced cellular uptake of cysteine, required for GSH synthesis, due to high levels of glutamate (Sagara and Schubert, 1998); (iv) decreased activity of enzymes involved in the GSH synthesis (e.g. glutathione synthetase) and/or recycling of GSSG via glutathione reductase; and (v) a diminished amount of NADPH, which is needed for GSSG reduction. However, regardless of the mechanism responsible for the decrease in low-molecular-mass thiols, GSH levels return to normal val-

ues in the chronic phase of the disease as inflammation also subsides. As expected, the amount of lipid peroxidation products is high in acute EAE and decreases to normal levels in the chronic phase. In contrast, protein carbonyls are also elevated in chronic EAE and are likely to be the result of the lower proteasome proteolytic activity in this stage of the disease. Thus cell death in the spinal cord of EAE mice exhibits a better temporal correlation with the build-up of oxidized proteins than with oxidative stress. Furthermore, although carbonyls are also present in live cells during the course of EAE, their levels are much higher in apoptotic cells, demonstrating a spatial correlation between these two parameters.

It is interesting to note that in both control and EAE spinal cord, astrocytes contain the highest levels of carbonyls, followed by oligodendrocytes and neurons. This result is not

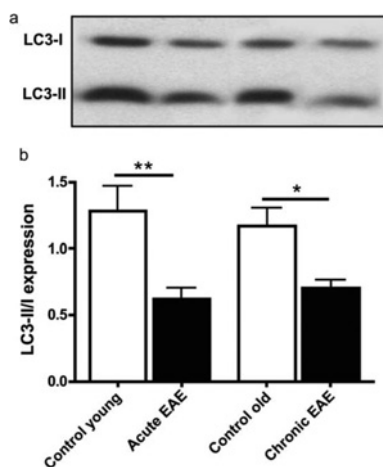


Figure 8 Autophagy is impaired in both acute and chronic EAE

(a) A representative Western blot depicting the expression of LC3-I and its shorter and lipidated form (LC3-II) in the spinal cord of control and EAE mice. (b) Autophagy index (i.e. LC3-II/LC3-I expression) was determined by densitometric scanning of the Western blots. Values represent the means \pm S.E.M. for four to six animals per experimental group. Clinical scores (means \pm S.E.M.) of acute and chronic EAE mice were 3.0 ± 0.3 and 2.8 ± 0.5 respectively. * $P < 0.05$, ** $P < 0.005$.

totally unexpected since astrocytes produce large levels of ROS (reactive oxygen species) (Keller et al., 1999) that could generate significant amounts of carbonyls within these cells. Nonetheless, it was somewhat surprising to find that the basal carbonyl staining in neurons and oligodendrocytes are significantly lower, particularly when these two cell types are considered to be highly susceptible to oxidative stress (Halliwell, 2006; Benarroch, 2009). Interestingly, the notion that astrocytes are less sensitive to oxidative damage than other CNS cells has been recently challenged. It has been found that astrocytes in the unperturbed mouse brain contain significantly lower levels of reduced glutathione than neurons and oligodendrocytes (Miller et al., 2009). An alternative possibility is that oligodendrocytes and neurons may have a more efficient proteolytic machinery to remove oxidized proteins thus reducing the build up of carbonylated proteins in these cells. Studies are underway to determine GSH and proteasome levels in individual cells during the course of EAE.

Carbonylation is known to cause inappropriate inter- and intra-protein cross-links as well as protein misfolding, which in turn results in the formation of high-molecular-mass aggregates (Grune et al., 1997; Mirzaei and Regnier, 2008). As these aggregates get larger they precipitate, become resistant to proteolytic degradation and reduce cell viability (Nyström, 2005; Maisonneuve et al., 2008a). The precise relationship between protein aggregate formation and apoptosis, or whether the aggregates are themselves cytotoxic, is unclear. It has been recently discovered that protein aggregates, as they form, sequester multiple pre-existent and newly synthesized proteins that have essential cellular functions and thus are critical for cell survival (Olzscha et al., 2011). The

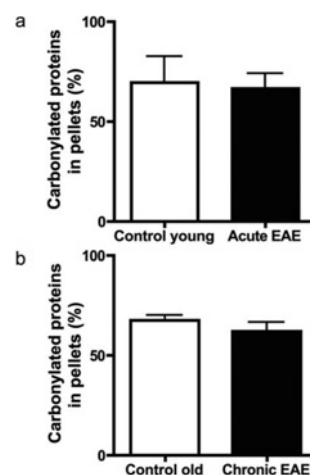


Figure 9 Carbonylated proteins partition into the aggregated protein fraction

Levels of protein carbonyls in the spinal cord homogenates and the Triton-insoluble aggregated protein fraction were quantified by oxyblot analysis. Values are expressed as the percentage of carbonylated proteins from the homogenate that are recovered in the aggregated protein fraction. Values represent the means \pm S.E.M. for three animals per experimental group. Clinical scores (means \pm S.E.M.) of acute and chronic EAE mice were 3.5 ± 0.0 and 2.2 ± 0.3 respectively. Note that although the amount of carbonylated proteins in EAE is much larger than in controls (Figure 4), the proportion of these oxidized species that partition into the aggregates is similar.

presence in EAE tissues of a significant number of cells containing large protein aggregates is noteworthy and may be due not only to an increase in the amount of carbonylated proteins, but also to a deficient removal. In this regard, we found that autophagy, the major mechanism for protein aggregate clearance (Son et al., 2012), is significantly reduced in both acute and chronic EAE, thereby explaining the presence of juxta-nuclear protein aggregates throughout the disease. While it is tempting to speculate that these inclusion bodies contribute significantly to cell death, there is some evidence suggesting aggresomes may instead provide a cytoprotective function by sequestering the toxic aggregated proteins (Tyedmers et al., 2010). Some of the same studies also propose that the smaller protein aggregates are the cytotoxic species. Thus, in the future, it will be important to determine the size-distribution of protein aggregates during the course of the disease as we may find that the presence of small rather than large aggregates correlates better with the changes in pathology and disease activity. Indeed, the occurrence in EAE of protein aggregates with a size smaller than those detected by histochemical analysis is very likely since protein carbonyls, which are enriched in the aggregates isolated by high-speed centrifugation, do not co-localize with the ProteoStat[®]-positive aggresomes and large cytoplasmic inclusion bodies.

Using neuronal cultures, we have recently found that a moderate depletion of glutathione (GSH), similar to that observed in EAE (the present study), leads to increased protein carbonylation, protein aggregation and cell death, all of

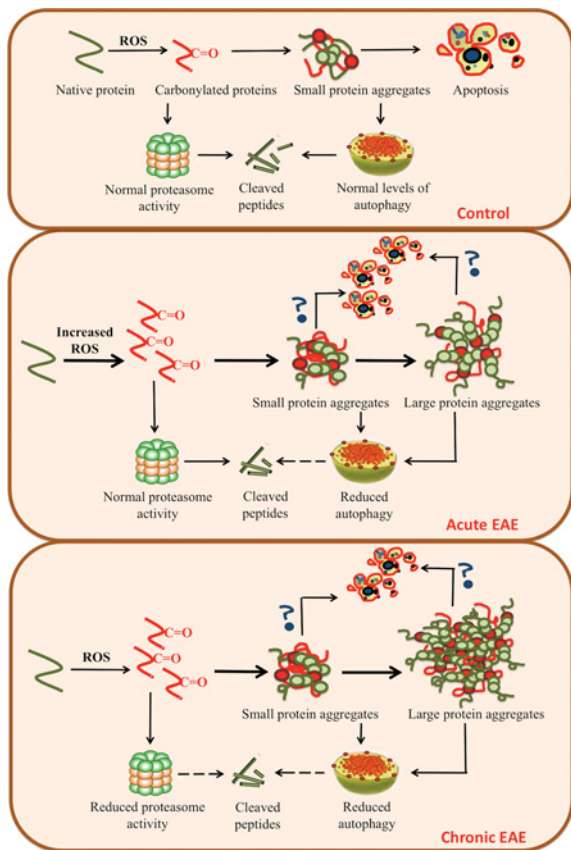


Figure 10 Schematic diagram that incorporates the major findings of the present study

Carbonylated proteins accumulate in the spinal cord of both acute and chronic EAE mice, albeit by different mechanisms: increased oxidative stress in acute EAE and decreased proteasomal activity in chronic EAE. Augmented protein carbonyl levels and diminished autophagy lead to the formation of protein aggregates throughout the course of the disease. The occurrence of small and/or large protein aggregates may be responsible for the increased neuronal and glial apoptosis. ROS, reactive oxygen species.

which are temporally correlated (Dasgupta et al., 2012). Furthermore, several protein carbonyl scavengers (hydralazine, histidine hydrazide and methoxylamine) prevented protein aggregation and cell death, suggesting that during GSH depletion oxidized proteins are critical for aggregate formation and cytotoxicity. In that study, we also found that protein aggregates are not made of carbonylated proteins exclusively since the cellular amount of oxidized species is approximately 1–2% of that of the aggregates. However, protein carbonylation may expose hydrophobic surfaces that can mediate aberrant interactions with other (non-oxidized) proteins, resulting in their functional impairment and sequestration as was recently proposed for several cerebral proteopathies (Walker and LeVine, 2012). Preliminary studies in our laboratory also show that inhibition of protein aggregation with Congo Red and 2-hydroxypropyl-β-cyclodextrin reduce neuronal cell death induced by partial GSH depletion without affecting oxidative stress or protein car-

bonylation, which suggests a direct link between protein oxidation, protein aggregation and cell death (A. Dasgupta and O.A. Bizzozero, unpublished work). In the future, it will be important to examine whether carbonyl scavengers and aggregation inhibitors prevent or reduce cell death and ameliorate disease activity in EAE. Interestingly, it has recently been found that the reactive carbonyl scavenger hydralazine reduces disease activity in acute EAE mice (Leung et al., 2011). Yet, while encouraging, these findings should be interpreted with caution since hydralazine is also a potent antioxidant (Zheng and Bizzozero, 2010b) and it is well known that reduction of oxidative stress ameliorates EAE (Marracci et al., 2002; Penkowa and Hidalgo, 2003; Hendricks et al., 2004; Offen et al., 2004). Studies using carbonyl scavengers lacking antioxidant and anti-inflammatory properties are thus needed to elucidate the role of protein oxidation in inflammatory demyelination.

FUNDING

This work was supported by the National Institutes of Health [PHHS grant NS057755].

REFERENCES

Arenella LS, Herndon R (1984) Mature oligodendrocytes: division following experimental demyelination in adult animals. *Arch Neurol* 41:1162–1165.

Akassoglou K, Bauer J, Kassiotis G, Pasparakis M, Lassmann H, Kollias G, Probert L (1998) Oligodendrocyte apoptosis and primary demyelination induced by local TNF/p55TNF receptor signaling in the central nervous system of transgenic mice models for multiple sclerosis with primary oligodendrogliopathy. *Am J Pathol* 153:801–813.

Aksenov MY, Aksenova MV, Butterfield DA, Geddes JW, Markesbery WR (2001) Protein oxidation in the brain in Alzheimer's disease. *Neuroscience* 103:373–383.

Anderson JM, Hampton DW, Patani R, Pryce G, Crowther RA, Reynolds R, Franklin RJM, Giovannoni G, Compston DA, Baker D, Spillantini MG, Chandran S (2008) Abnormally phosphorylated tau is associated with neuronal and axonal loss in experimental autoimmune encephalomyelitis and multiple sclerosis. *Brain* 131:1736–1748.

Benarroch EE (2009) Oligodendrocytes: susceptibility to injury and involvement in neurologic disease. *Neurology* 72:1779–1785.

Bizzozero OA (2009) Protein carbonylation in neurodegenerative and demyelinating CNS diseases. In *Handbook of Neurochemistry and Molecular Neurobiology* (Lajtha A, Banik N, Ray S, eds), pp. 543–562, Springer.

Bizzozero OA, DeJesus G, Callahan K, Pastuszyn A (2005) Elevated protein carbonylation in the brain white matter and gray matter of patients with multiple sclerosis. *J Neurosci Res* 81:687–695.

Dalle-Donne I, Rossi R, Giustarini D, Gagliano N, Lusini L, Milzani A, Di Simplicio P, Colombo R (2001) Actin carbonylation: from a simple marker of protein oxidation to relevant signs of severe functional impairment. *Free Radical Biol Med* 31:1075–1083.

Das A, Guyton MK, Matzelle DD, Ray SK, Banik NL (2008) Time-dependent increases in protease activities for neuronal apoptosis in spinal cords of Lewis rats during development of acute experimental autoimmune encephalomyelitis. *J Neurosci Res* 86:2992–3001.

- Dasgupta A, Bizzozero OA (2011) Positive correlation between protein carbonylation and apoptosis in EAE. *Trans Am Soc Neurochem* 42:PSM08-01.
- Dasgupta A, Zheng J, Bizzozero OA (2012) Protein carbonylation and aggregation precede neuronal apoptosis induced by partial glutathione depletion. *ASN NEURO* 4(3):art:e00084.doi:10.1042/AN20110064.
- Divald A, Powell S (2006) Proteasome mediates removal of proteins oxidized during myocardial ischemia. *Free Radical Biol Med* 4:156-164.
- England K, O'Driscoll C, Cotter TG (2004) Carbonylation of glycolytic proteins is a key response to drug-induced oxidative stress and apoptosis. *Cell Death Differ* 11:252-260.
- Ferrante RJ, Browne SE, Shinobu LA, Bowling AC, Baik MJ, MacGarvey U, Kowall NW, Brown RH, Beal MF (1997) Evidence of increased oxidative damage in both sporadic and familial amyotrophic lateral sclerosis. *J Neurochem* 69:2064-2074.
- Ferrington DA, Husom AD, Thompson LV (2005) Altered proteasome structure, function and oxidation in aged muscle. *FASEB J* 19:644-646.
- Floor E, Wetzell MG (1998) Increased protein oxidation in human substantia nigra pars compacta in comparison with basal ganglia and prefrontal cortex measured with an improved dinitrophenylhydrazine assay. *J Neurochem* 70:268-275.
- Fucci L, Oliver CN, Coon MJ, Stadtman ER (1983) Inactivation of key metabolic enzymes by mixed-function oxidation reactions: possible implication in protein turnover and ageing. *Proc Nat Acad Sci USA* 80:1521-1525.
- Gilgun-Sherki Y, Melamed E, Offen D (2004) The role of oxidative stress in the pathogenesis of multiple sclerosis: the need for effective antioxidant therapy. *J Neurol* 251:261-268.
- Gold R, Hartung HP, Toyka KV (2000) Animal models for autoimmune demyelinating disorders of the nervous system. *Mol Med Today* 6:88-91.
- Grune T, Reinheckel T, Davies KJ (1997) Degradation of oxidized proteins in mammalian cells. *FASEB J* 11:526-534.
- Guyton MK, Wingrave JM, Yallapragada AV, Wilford GG, Sribnick EA, Matzelle DD, Tyor WR, Ray SK, Banik NL (2005) Upregulation of calpain correlates with increased neurodegeneration in acute experimental autoimmune encephalomyelitis. *J Neurosci Res* 81:53-61.
- Haider L, Fischer MT, Frischer JM, Bauer J, Höftberger R, Botond G, Esterbauer H, Binder CJ, Witztum JL, Lassmann H (2011) Oxidative damage in multiple sclerosis lesions. *Brain* 134:1914-1924.
- Halliwel B (2006) Oxidative stress and neurodegeneration: where are we now? *J Neurochem* 97:1634-1658.
- Hassen GW, Feliberti J, Kesner L, Stracher A, Mokhtarian F (2006) A novel calpain inhibitor for the treatment of acute experimental autoimmune encephalomyelitis. *J Neuroimmunol* 180:135-146.
- Hendriks JJ, Alblas J, van der Pol SM, van Tol EA, Dijkstra CD, de Vries HE (2004) Flavonoids influence monocytic GTPase activity and are protective in experimental allergic encephalitis. *J Exp Med* 200:1667-1672.
- Keller JN, Hanni KB, Gabbita SP, Friebe V, Mattson MP, Kindy MS (1999) Oxidized lipoproteins increase reactive oxygen species formation in microglia and astrocyte cell lines. *Brain Res* 830:10-15.
- Keller JN, Hanni KB, Marksberry WR (2000) Impaired proteasome function in Alzheimer's disease. *J Neurochem* 75:436-439.
- Kornek B, Lassmann H (1999) Axonal pathology in multiple sclerosis: a historical note. *Brain Pathol* 9:651-656.
- Kuerten S, Kostova-Bales DA, Frenzel LP, Tigno JT, Tary-Lehmann M, Angelov DN, Lehmann PV (2007) MP4- and MOG:35-55-induced EAE in C57BL/6 mice differentially targets brain, spinal cord and cerebellum. *J Neuroimmunol* 189:31-40.
- Leung G, Sun W, Zheng L, Brookes S, Tully M, Shi R (2011) Anti-acrolein treatment improves behavioral outcome and alleviates myelin damage in experimental autoimmune encephalomyelitis mouse. *Neuroscience* 173:150-155.
- Lucchinetti CF, Bruck W, Rodriguez M, Lassmann H (1996) Distinct patterns of multiple sclerosis pathology indicate heterogeneity in pathogenesis. *Brain Pathol* 6:259-274.
- Luo S, Wehr NN (2009) Protein carbonylation: avoiding pitfalls in the 2,4-dinitrophenylhydrazine assay. *Redox Rep* 14:159-166.
- McNaught KS, Belizaire R, Isacson O, Jenner P, Olanow CW (2003) Altered proteasomal function in sporadic Parkinson's disease. *Exp Neurol* 179:38-46.
- Magi B, Ettore A, Liberatori S, Bini L, Andreassi M, Frosali S, Neri P, Pallini V (2004) Selectivity of protein carbonylation in the apoptotic response to oxidative stress associated with photodynamic therapy: a cell biochemical and proteomic investigation. *Cell Death Differ* 11:842-852.
- Maisonneuve E, Ezraty B, Dukan S (2008a) Protein aggregates: an aging factor involved in cell death. *J Bacteriol* 190:6070-6075.
- Maisonneuve E, Fraysse L, Lignon S, Capron L, Dukan S (2008b) Carbonylated proteins are detectable only in a degradation-resistant aggregate state in *Escherichia coli*. *J Bacteriol* 190:6609-6614.
- Marracci GH, Jones RE, McKeon GP, Bourdette DN (2002) α -Lipoic acid inhibits T cell migration into the spinal cord and suppresses and treats experimental autoimmune encephalomyelitis. *J Neuroimmunol* 131:104-114.
- Meyer R, Weissert R, Diem R, Storch MK, de Graaf KL, Kramer B, Bahr M (2001) Acute neuronal apoptosis in a rat model of multiple sclerosis. *J Neurosci* 21:6214-6220.
- Miller VM, Lawrence DA, Mondal TK, Seegal RF (2009) Reduced glutathione is highly expressed in white matter and neurons in the unperturbed brain: implication for oxidative stress associated with neurodegeneration. *Brain Res* 1276:22-30.
- Mirzaei H, Regnier F (2008) Protein:protein aggregation induced by protein oxidation. *J Chromatogr* 873:8-14.
- Müller DM, Pender MP, Greer JM (2000) A neuropathological analysis of experimental autoimmune encephalomyelitis with predominant brain stem and cerebellar involvement and differences between active and passive induction. *Acta Neuropathol* 100:174-182.
- Nyström T (2005) Role of oxidative carbonylation in protein quality control and senescence. *EMBO J* 24:1311-1317.
- Offen D, Gilgun-Sherki Y, Barhum Y, Benhar M, Grinberg L, Reich R, Melamed E, Atlas D (2004) A low molecular weight copper chelator crosses the blood-brain barrier and attenuates experimental autoimmune encephalomyelitis. *J Neurochem* 89:1241-1251.
- Ohkawa H, Ohishi N, Yagi K (1979) Assay for lipid peroxides in animal tissues by thiobarbituric acid reaction. *Anal Biochem* 95:331-358.
- Olzsha H, Schermann SM, Woerner AC, Pinket S, Hecht MH, Tartaglia GG, Vendruscolo M, Hayer-Hartl M, Hartl FU, Vabulas RM (2011) Amyloid-like aggregates sequester numerous metastable proteins with essential cellular functions. *Cell* 144:67-78.
- Pender MP, Nguyen KB, McCombe PA, Kerr JF (1991) Apoptosis in the nervous system in experimental allergic encephalomyelitis. *J Neurol Sci* 104:81-87.
- Penkowa M, Hidalgo J (2003) Treatment with metallothionein prevents demyelination and axonal damage and increases oligodendrocyte precursors and tissue repair during experimental autoimmune encephalomyelitis. *J Neurosci Res* 72:574-586.
- Perluigi M, Poon HF, Maragos W, Pierce WM, Klein JB, Calabrese V, Cini C, DeMarco C, Butterfield DA (2005) Proteomic analysis of protein expression and oxidative modification in R6/2 transgenic mice: a model of Huntington's disease. *Mol Cell Proteomics* 4:1849-1861.
- Rodgers KJ, Dean RT (2003) Assessment of proteasome activity in cell lysates and tissue homogenates using peptide substrates. *Int J Biochem Cell Biol* 35:716-727.
- Sagara Y, Schubert D (1998) The activation of metabotropic glutamate receptors protects nerve cells from oxidative stress. *J Neurosci* 18:6662-6671.
- Seo H, Sonntag KC, Isacson O (2004) Generalized brain and skin proteasome inhibition in Huntington's disease. *Ann Neurol* 56:319-328.
- Shaik IH, Mehvar R (2006) Rapid determination of reduced and oxidized glutathione levels using a new thiol-masking reagent and the enzymatic recycling method: application to the rat liver and bile samples. *Anal Bioanal Chem* 385:105-113.
- Shringarpure R, Grüne T, Davies KJ (2001) Protein oxidation and 20S proteasome-dependent proteolysis in mammalian cells. *Cell Mol Life Sci* 58:1442-1450.
- Smerjac SM, Bizzozero OA (2008) Cytoskeletal protein carbonylation and degradation in experimental autoimmune encephalomyelitis. *J Neurochem* 105:763-772.

- Smith KJ, Kapoor R, Felts PA (1999) Demyelination: the role of reactive oxygen and nitrogen species. *Brain Pathol* 9:69–92.
- Son JH, Shim JH, Kim KH, Ha JY, Han JY (2012) Neuronal autophagy and neurodegenerative diseases. *Exp Mol Med* 44:89–98.
- Stadtman ER, Berlett BS (1997) Reactive oxygen-mediated protein oxidation in aging and disease. *Chem Res Toxicol* 10:485–494.
- Starke PE, Oliver CN, Stadtman ER (1987) Modification of hepatic proteins in rats exposed to high oxygen concentration. *FASEB J* 1:36–39.
- Toft-Hansen H, Füchtbauer L, Owens T (2011) Inhibition of reactive astrocytosis in established experimental autoimmune encephalomyelitis favors infiltration by myeloid cells over T cells and enhances severity of disease. *Glia* 59:166–176.
- Tripathi RB, Rivers LE, Young KM, Jamen F, Richardson WD (2010) PDGFRA/NG2 glia generate new oligodendrocytes but few astrocytes in a murine EAE model of demyelinating disease. *J Neurosci* 30:16383–16390.
- Tyedmers J, Mogk A, Bukau B (2010) Cellular strategies for controlling protein aggregation. *Nat Rev* 11:777–788.
- Vogt J, Paul F, Aktas O (2009) Lower motor neuron loss in multiple sclerosis and experimental autoimmune encephalomyelitis. *Ann Neurol* 66:310–322.
- Walker LC, LeVine H (2012) Corruption and spread of pathogenic proteins in neurodegenerative diseases. *J Biol Chem* 287:33109–33115.
- Zheng J, Bizzozero OA (2010a) Accumulation of protein carbonyls within cerebellar astrocytes in murine experimental autoimmune encephalomyelitis. *J Neurosci Res* 88:3376–3385.
- Zheng J, Bizzozero OA (2010b) Reduced proteasomal activity contributes to the accumulation of carbonylated proteins in chronic experimental autoimmune encephalomyelitis. *J Neurochem* 115:1556–1567.
- Zheng J, Bizzozero OA (2011) Decreased activity of the 20S proteasome in the brain white matter and gray matter of patients with multiple sclerosis. *J Neurochem* 117:143–153.
- Zheng J, Dasgupta A, Bizzozero OA (2012) Changes in 20S subunit composition are largely responsible for altered proteasomal activities in experimental autoimmune encephalomyelitis. *J Neurochem* 121:486–494.

Received 12 December 2012/4 March 2013; accepted 14 March 2013

Published as Immediate Publication 14 March 2013, doi 10.1042/AN20120088

Increased carbonylation, protein aggregation and apoptosis in the spinal cord of mice with experimental autoimmune encephalomyelitis

Anushka Dasgupta*, Jianzheng Zheng*, Nora I. Perrone-Bizzozero† and Oscar A. Bizzozero*¹

*Department of Cell Biology and Physiology, University of New Mexico Health Sciences Center, Albuquerque, NM, U.S.A.

†Department of Neurosciences, University of New Mexico Health Sciences Center, Albuquerque, NM, U.S.A.

SUPPLEMENTARY DATA

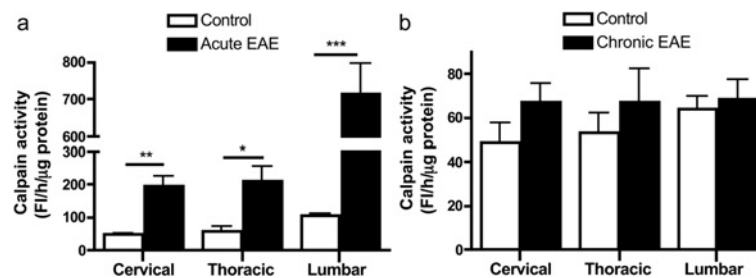


Figure S1 Calpain activity is increased only in acute EAE (a and b) Calpain activity in the different mouse spinal cord regions (cervical, thoracic and lumbar) in acute and chronic EAE respectively. FI, fluorescence intensity. Values represent the means \pm S.E.M. for four to five animals per experimental group. Clinical scores (means \pm S.E.M.) of acute and chronic EAE mice were 2.3 ± 0.5 and 2.7 ± 0.5 respectively. * $P < 0.05$, ** $P < 0.005$, *** $P < 0.0005$.

¹To whom correspondence should be addressed (email obizzozero@salud.unm.edu).